The Journal of Immunology

Lipid Rafts Mediate Association of LFA-1 and CD3 and Formation of the Immunological Synapse of CTL

Muhammad Reza Marwali, Matthew A. MacLeod, David N. Muzia and Fumio Takei

J Immunol 2004; 173:2960-2967; ;
doi: 10.4049/jimmunol.173.5.2960
http://www.jimmunol.org/content/173/5/2960

The Journal of Immunology is published twice each month by
The American Association of Immunologists, Inc.,
1451 Rockville Pike, Suite 650, Rockville, MD 20852

Print ISSN: 0022-1767 Online ISSN: 1550-6606.

Lipid Rafts Mediate Association of LFA-1 and CD3 and Formation of the Immunological Synapse of CTL[1]

Muhammad Reza Marwali,* Matthew A. MacLeod,* David N. Muzia,* and Fumio Takei[2]*†

Lipid rafts accumulate in the immunological synapse formed by an organized assembly of the TCR/CD3, LFA-1, and signaling molecules. However, the precise role of lipid rafts in the formation of the immunological synapse is unclear. In this study, we show that LFA-1 on CTL is constitutively active and mediates Ag-independent binding of CTL to target cells expressing its ligands. LFA-1 and CD3 on CTL, but not resting T cells, colocalize in lipid rafts. Binding of LFA-1 on CTL to targets initiates the formation of the immunological synapse, which is formed by LFA-1, CD3, and ganglioside GM1 distributed in the periphery of the cell contact site and cholesterol is more widely distributed. The formation of this synapse is Ag independent, but the recognition of Ag by the TCR induces accumulation of tyrosine phosphorylated proteins in the synapse as well as redistribution of the microtubule organization center toward the cell contact site. Our results suggest that LFA-1 recruits lipid rafts and the TCR/CD3 to the synapse, and facilitates efficient and rapid activation of CTL. ***The Journal of Immunology*****, 2004, 173: 2960–2967.**

Lipid rafts are plasma membrane microdomains that are rich in sphingolipids with saturated acyl chains and cholesterol in the outer leaflet (1). They are insoluble in cold, nonionic detergents and can be isolated in detergent-insoluble low-density fractions in sucrose gradient centrifugation. Lipid rafts are thought to be important for cell signaling and membrane trafficking because certain surface receptors and signaling molecules localize in lipid rafts (2). Recent reports suggest that lipid rafts in T cells do not simply exist as one distinct type of membrane microdomain but rather they may be heterogeneous (3–5). On primary resting T cells, lipid rafts can be divided into ganglioside GM1-rich and cholesterol-rich domains (4). LFA-1 on resting T cells associates with cholesterol-rich rafts, whereas Lck and Thy-1 associate with GM1-rich rafts. The significance of the heterogeneity of lipid rafts in T cell functions is still unclear.

The immunological synapse is a supra-molecular structure that is formed in the contact area between T cell and APC (6). In mature synapse, LFA-1 is found to form an outer ring called the peripheral supra-molecular activation cluster and the TCR and signaling molecules are in the center supra-molecular activation cluster (7–9). The mature synapse lasts for several hours and is thought to be important for sustained TCR signaling (10). At the same time, TCR signaling seems to be important for the maintenance of the immunological synapse (11–14). The immunological synapse formed upon CTL-target cell interaction has also been reported. Similar to the synapse formed in resting T cell-APC interaction, the CTL synapse also has LFA-1 in the periphery with a secretory domain in the center (15, 16). However, unlike activation of resting T cell, which requires prolonged activation, CTL becomes activated and releases cytotoxic granules within minutes following recognition of appropriate targets. Therefore, the activation machinery in CTL may be preassembled before target cell recognition.

Lipid rafts accumulate in the immunological synapse (17–19). This has been demonstrated by staining of GM1 with fluorescent cholera toxin (17, 19). However, the mechanisms by which lipid rafts accumulate in the immunological synapse are unknown. Moreover, lipid rafts are heterogeneous, and some cholesterol-rich rafts of T cells contain little GM1. Conversely, cholesterol depletion with methyl-β-cylodextrin (MCD),[3] which is often used to disrupt lipid rafts, does not disrupt GM1-rich lipid rafts. Thus, the heterogeneity of lipid rafts complicates our understanding of their role in the formation of the immunological synapse.

We have examined the role of lipid rafts in formation of the immunological synapse of CTL. Our results show that the formation of the immunological synapse of CTL is different from that of resting T cells. CD3 on CTL, but not resting T cells, localizes in lipid rafts and associates with LFA-1, which is already in a high-avidity state and readily mediates the binding of CTL to target cells. Through the association with LFA-1, the TCR/CD3 complex is recruited to the contact site to form the CTL immunological synapse independent of Ag/MHC recognition. Within the immunological synapse, LFA-1, CD3, and GM1 remain in the periphery whereas cholesterol is more widely distributed.

Materials and Methods

Mice, cells, Abs, and reagents

C57BL/6 mice were obtained from The Jackson Laboratory (Bar Harbor, ME) and H-Y TCR transgenic Rag-$2^{-/-}$ C57BL/10 mice were obtained from Taconic Farms (Tarrytown, NY). These mice were bred in the Joint Animal Facility of the BC Cancer Research Centre (Vancouver, British Columbia, Canada). Splenic T cells were isolated by the murine T cell enrichment kit, SpinSep (StemCell Technologies, Vancouver, British Columbia, Canada), as described (4). The murine lymphoma line RMA and the murine fibroblast L cells were from American Type Culture Collection (ATCC, Rockville, MD). Rat anti-murine CD18 hybridomas (TIB213 and TIB218) and mouse anti-D^b hybridoma (28-8-6S) were also from the ATCC. FITC-conjugated anti-CD3ϵ and PE-conjugated anti-CD11c Abs were purchased from BD Biosciences (San Diego, CA). The YN1/1 mAb specific for murine ICAM-1 has been described (20). Mouse anti-Lck

*Terry Fox Laboratory, BC Cancer Agency, Vancouver, British Columbia, Canada; and †Department of Pathology and Laboratory Medicine, Faculty of Medicine, University of British Columbia, Vancouver, British Columbia, Canada

Received for publication January 20, 2004. Accepted for publication June 17, 2004.

The costs of publication of this article were defrayed in part by the payment of page charges. This article must therefore be hereby marked *advertisement* in accordance with 18 U.S.C. Section 1734 solely to indicate this fact.

[1] This work was supported by a grant from the Canadian Institutes of Health Research.

[2] Address correspondence and reprint requests to Dr. Fumio Takei, Terry Fox Laboratory, BC Cancer Research Centre, 601 West 10th Avenue, Vancouver, British Columbia, V5Z 1L3, Canada. E-mail address: ftakei@bccrc.ca

[3] Abbreviations used in this paper: MCD, methyl-β-cyclodextrin; CtxB, cholera toxin B subunit; MTOC, microtubule organizing center; 3-D, three-dimensionally.

0022-1767/04/$02.00

(3A5) and anti-CD3ζ (6B10.2) mAbs were from Santa Cruz Biotechnology (Santa Cruz, CA). Anti-phosphotyrosine mouse Ab (clone 4G10) was from Upstate (Lake Placid, NY) and anti-β-tubulin mouse Ab was from Chemicon International (Temecula, CA). HRP-conjugated cholera toxin B subunit (CtxB), FITC-conjugated CtxB, biotin-conjugated CtxB, MCD, filipin III, water-soluble cholesterol (MCD-cholesterol complex), BSA fragment V, Triton-X100, Brij 35, protease inhibitors (leupeptin, phenyl-methyl-succinyl fluoride, aprotinin, and pepstatin A), and $NaVO_4$ and $NaMoO_4$ were from Sigma-Aldrich (St. Louis, MO). Murine recombinant soluble ICAM-1 has been described (21). Calcein-AM, Alexa Fluor 568-, Alexa Fluor 647-, and Alexa Fluor 488-conjugated goat anti-rat Ig secondary Abs, Alexa Fluor 568-conjugated streptavidin, Alexa Fluor 568-, and Alexa Fluor 488-conjugated goat anti-mouse were from Molecular Probes (Eugene, OR). H-Y peptide (KCSRNRQYL) and control randomized H-Y peptide (NYQRSLCKR) were generated in the Nucleic Acids Protein Services facility of the University of British Columbia (Vancouver, British Columbia, Canada).

Transfection

L cells were transfected with mouse ICAM-1 cDNA in the pBCMGS expression vector and selected with G418 (22). L cells were also cotransfected with a genomic DNA fragment encoding MHC class I D^b (a gift from Dr. W. Jefferies, University of British Columbia) and the pRC42 plasmid (a gift from Dr. R. Kay, Terry Fox Laboratory, Vancouver, British Columbia, Canada) carrying a hygromycin-resistance gene and selected with hygromycin. For coexpression of D^b and ICAM-1, D^b-transfected L cells were further transfected with ICAM-1 and selected with both G418 and hygromycin. All the transfections were done using Lipofectamine Plus (Invitrogen Life Technologies, Burlington, Ontario, Canada) according to the manufacturer's instructions. The transfected cells were stained with appropriate Abs and sorted to establish L cell lines expressing high levels of D^b and/or ICAM-1.

Preparation of CTL

Dendritic cells were isolated from the spleen of male C57BL/6 (6- to 8-wk-old) mice using anti-CD11c-PE conjugated as primary Ab then separated by using an Easy Sep PE selection kit from StemCell Technologies. Splenocytes and lymph node cells (6×10^6/ml) from female H-Y TCR transgenic Rag-$2^{-/-}$ C57BL/10 mice were stimulated with irradiated (30 Gy) dendritic cells, 10:1 ratio, in total cells of $6–8 \times 10^6$/ml in 2.5 ml medium in the presence of 20 U/ml IL-2 in RPMI 1640 medium supplemented with 10% FCS, 2 mM L-glutamine, 5×10^{-5} M 2-ME, and penicillin/streptomycin for 5–6 days in 12-well culture plates.

Cholesterol depletion and reconstitution

For cholesterol depletion, cells were treated with various concentrations of MCD in HBSS containing 50 mM HEPES for 30 min at 37°C. To reconstitute cholesterol of MCD-treated cells, 60 μg/ml water-soluble cholesterol in HBSS containing 0.2% BSA was added to the cells and incubated for 30 min at 37°C.

Cell adhesion assay

LFA-1-mediated cell adhesion to immobilized soluble ICAM-1 was assayed as described (4). Briefly, cells labeled with calcein-AM were incubated in microwells coated with soluble ICAM-1 for 30 min at 37°C. Nonadherent cells were washed away, and the fluorescence intensities of the cells before and after the wash were measured by CytoFluor 2300 (Millipore, Bedford, MA). The percentages of cell adhesion were determined by the ratio of the fluorescence values of postwash over prewash after subtracting the background fluorescence values. For stimulation of LFA-1, cells were preincubated with 50 ng/ml PMA for 30 min at 37°C. For specificity control, anti-LFA-1 mAb (TIB 213) was also added. For the cholesterol depletion, MCD was added to cells as they were treated with PMA.

Sucrose gradient centrifugation and Western blotting

Cells (5×10^7) were washed twice with PBS and lysed in 1 ml ice-cold lysis buffer containing 20 mM Tris-HCl (pH 7.2), 150 mM KCl, various concentrations of nonionic detergents, and protease inhibitors. The cell lysates were sheared by five successive passages through 26-gauge hypodermic needles, then mixed with an equal volume of 80% sucrose (w/v) in ice-cold lysis buffer without detergent and transferred to SW41 centrifuge tubes. The samples were then overlaid with 6 ml of 30% sucrose and 3.5 ml of 5% sucrose and centrifuged (Beckman Coulter, Palo Alto, CA) at $200,000 \times g$ for 18 h. Protease inhibitors, $NaVO_4$ and $NaMoO_4$, were added to the gradients. All the procedures were done at 4°C. Following centrifugation, eight fractions of 1.5 ml each were collected, starting at the top of the gradient. Fractions 2 and 3 corresponding to the 5–30% sucrose interface were referred to as low-density fractions. Fractions 7 and 8 were referred to as high-density fractions. The materials at the bottom of the tube were referred to as pellet. Aliquots of each fraction were boiled in SDS-PAGE sample buffer (nonreducing condition), loaded onto SDS-PAGE, and transferred to polyvinylidene fluoride transfer membrane (Pall Gelman Laboratory, Ann Arbor MI). Proteins on the blots were detected by specific Abs and visualized by chemiluminescence by an ECL system (Amersham Biosciences, Piscataway, NJ) according to the manufacturer's protocols.

Cytotoxicity assay

RMA cells were pulsed with 1 μM H-Y peptide at 37°C for 2–3 h, washed, and incubated with 100 μCi of ^{51}Cr-sodium chromate (NEN, Boston, MA) for 1 h at 37°C. CTL were either treated with MCD or not, or treated with MCD and replenished with cholesterol. After washing twice, the radiolabeled target and effector cells were mixed at the indicated E:T ratio in RPMI 1640 0.2% BSA in a final volume of 200 μl in a U-bottom 96-well plate and incubated for 4 h at 37°C. Supernatants (100 μl) were collected and radioactivities were measured by a gamma-scintillation counter. The percentages of specific lysis were calculated as a percentage of lysis = ((cpm sample) − (cpm spontaneous release))/((cpm total) − (cpm spontaneous release)) × 100. Each cytotoxicity assay was done in triplicate.

Flow cytometry

Single cell suspensions of mouse fibroblast L cells were prepared by incubation of monolayer cultures with 5 mM EDTA in HBSS and stained with rat anti-mouse ICAM-1 mAb (10 μg/ml), mouse anti-D^b mAb (10 μg/ml), or both for 30 min on ice. After washing, FITC-conjugated anti-mouse-IgG and Alexa Fluor 647-conjugated anti rat-IgG secondary Abs were added and incubated for an additional 30 min. The stained cells were washed and analyzed by a FACScan flow cytometer (BD Biosciences). The purity of CTL generated in vitro was assessed by staining with FITC-conjugated anti-CD3ε Ab.

Fluorescence microscopy

For cocapping experiments, cells were incubated at 4°C with 10 μg/ml anti-LFA-1 mAb (TIB 213), 10 μg/ml FITC-conjugated anti-CD3ε Ab, 15 μg/ml FITC-CtxB, or 125 μg/ml filipin where indicated. After washing, cells were then incubated with Alexa Fluor 568-conjugated, Alexa Fluor 647-, or Alexa Fluor 488-conjugated goat anti-rat Ig for LFA-1 staining, and capping was induced by incubation at 37°C for 30 min, followed by fixation with 4% formaldehyde. For capping of GM1, cells were incubated with CtxB-biotin, washed, and stained with Alexa Fluor 568-conjugated streptavidin. The stained cells were cross-linked with rabbit anti-cholera toxin sera (Sigma-Aldrich) and incubated at 37°C for 30 min. Cells were cytospun onto poly-L-lysine-coated glass cover slips and analyzed by confocal microscopy (Radiance 2000 Multiphoton; Bio-Rad, Hercules, CA) equipped with Kr and Mai Tai Ti Sapphire lasers (SpectroPhysics, Mountain View, CA) and ×60 objective lens. Filipin III was excited with a multi-photon laser at 779 nm and the emission filter was HQ 450/80 with a BGG 22 blocking filter. FITC was excited by 488 nm and the emission filter was HQ 515/30. Alexa 568 was excited by 568 nm and the emission filter was HQ 600/50. Signals were collected sequentially to avoid bleed-through.

For immunological synapse experiments, L cells were grown on gelatin-coated coverslips overnight. The following day, CTLs were added to the L cells after pulsing with 1 μM H-Y peptide and incubated at 37°C for 5, 15, and 20 min after brief centrifugation. The cells were then fixed with 4% paraformaldehyde. After washing, the cells were blocked with PBS containing BSA. The fixed cells were stained with various combinations of FITC-conjugated CtxB or biotin-conjugated CtxB, anti-LFA-1, and FITC-conjugated anti-CD3ε Abs and incubated at room temperature for 1 h. After washing twice, Alexa Fluor 568-conjugated anti-rat Ab or Alexa Fluor 568-conjugated streptavidin was added and incubated for 1 h at room temperature. The cells were washed twice with HBSS and incubated with 125 μg/ml filipin III on ice for 1 h. After washing, the stained cells were mounted on Vectashield (Vector Laboratories, Burlingame, CA). Conjugates were examined with a deconvolution microscope (Deltavision, Seattle, WA) with z steps 0.1 μm and 10 iterations. Images were processed by the Softworx software program (Deltavision). Stacks were three-dimensionally (3-D) reconstructed, and the CTL-L cell interphase was cropped and rotated to obtain a view from the CTL side using Volocity software (Improvision, Lexington, MA).

Results

Lipid rafts are important for cytotoxicity of CTL

Lymphocytes from female H-Y-specific TCR transgenic Rag-$2^{-/-}$ mice were stimulated with male dendritic cells to generate CTL specific for the H-Y peptide presented by D^b. The CTL thus generated are almost pure (Fig. 1*A*) and effectively killed the murine lymphoma line RMA (H-2^b) pulsed with the H-Y peptide, but not with control randomized peptide or with no peptide (Fig. 1*B*). To examine the role of lipid rafts in cytotoxicity of CTL, we disrupted lipid rafts by extracting cholesterol with MCD (23). The maximum concentration of MCD that did not cause cell death of CTL, as determined by trypan blue staining, was 20 mM. At this concentration, MCD strongly inhibited cytotoxicity of CTL (Fig. 1*B*) and this inhibition was reversed by cholesterol reconstitution, indicating the specificity of MCD treatment. The treatment of CTL with 20 mM MCD removed 50% of membrane cholesterol but did not affect the level of GM1 as determined by flow cytometric analysis (data not shown). Therefore, lipid rafts seem to be important for cytotoxicity of CTL.

Next we tested whether this inhibition was due to inhibition of LFA-1. We have previously shown that LFA-1-mediated adhesion of resting T cells is strongly inhibited by MCD (4). LFA-1 on CTL was significantly different from that on resting T cells. The former seemed to be already in an active state and readily mediated adhesion of CTL to ICAM-1 (Fig. 1*C*), whereas LFA-1 on resting T cells had to be activated to mediate adhesion (Fig. 1*D*). Furthermore, the adhesion of CTL to ICAM-1 was relatively resistant to MCD. Even with 20 mM MCD, which killed resting T cells, the adhesion of CTL was only partially inhibited, whereas LFA-1-mediated adhesion of resting T cells was almost completely inhibited with 10 mM MCD. Therefore, it is unlikely that the inhibition of the cytotoxicity of CTL with MCD was due to inhibition of adhesion of CTL to target cells (24). It is more likely that TCR-mediated signaling events may be inhibited by cholesterol depletion with MCD.

LFA-1 and CD3 on CTL localize in MCD-sensitive lipid rafts

To examine the distribution of LFA-1 and CD3 in lipid rafts, CTL and resting T cells were lysed with cold, nonionic detergent Brij 35 (1%) followed by sucrose gradient ultracentrifugation, and individual fractions were analyzed by Western blotting. The low-density fractions contained detergent-insoluble lipid rafts, as indicated by the presence of ganglioside GM1, a commonly used marker for lipid rafts. Approximately 60% of LFA-1 on CTL and 50% on resting T cells were found in the detergent-insoluble low-density lipid raft fractions (Fig. 2). Cholesterol depletion with MCD shifted ~50% of LFA-1 in the raft fractions to detergent-soluble nonraft fractions, indicating that half of LFA-1 in lipid rafts is

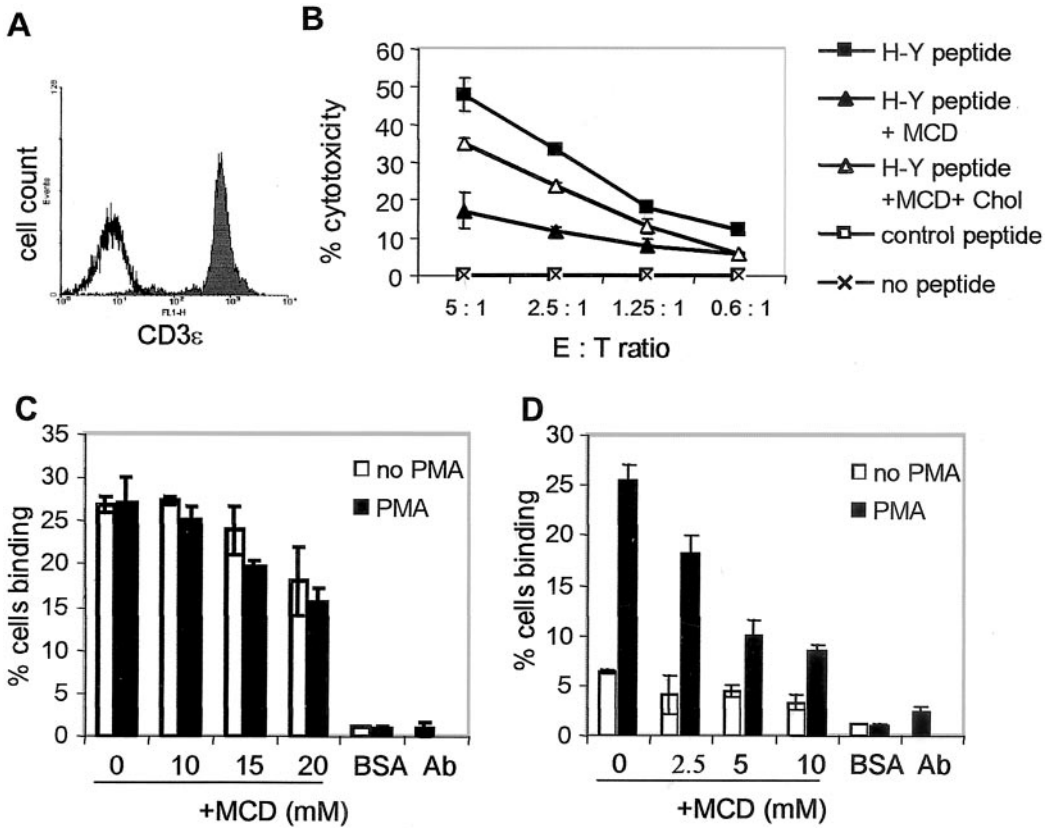

FIGURE 1. Cholesterol depletion inhibits CTL cytotoxicity. CTL was generated from H-Y TCR transgenic Rag-$2^{-/-}$ mice as described in *Materials and Methods*. *A*, CTL was analyzed for purity by flow cytometry. Open histogram shows staining with isotype control Ab and solid histogram shows staining with FITC-conjugated anti-CD3ϵ Ab. *B*, Cytotoxicity of CTL was analyzed by ^{51}Cr-release assay using RMA cells as target. RMA cells were pulsed with H-Y peptide (■), control peptide (□), or no peptide (×). Some CTLs were treated with 20 mM MCD at 37°C for 30 min (▲) to deplete cholesterol or cholesterol-depleted and reconstituted with 60 μg/ml water-soluble cholesterol (Chol) at 37°C for an additional 30 min (△), and tested against H-Y-peptide-pulsed RMA cells. *C*, CTLs were fluorescence-labeled with calcein-AM, treated with an indicated concentration of MCD for 30 min, and then incubated with (filled bars) or without (open bars) 50 ng/ml PMA for 30 min at 37°C in serum-free HBSS. The adhesion of the treated cells to ICAM-1 was determined as described in *Materials and Methods*. Anti-LFA-1 Ab (10 μg/ml) was added to inhibit cell adhesion to confirm LFA-1-dependent cell adhesion, and BSA-coated wells were used as control. *D*, Adhesion of primary splenic T cells to ICAM-1 was tested as above. The results are representative of three independent experiments.

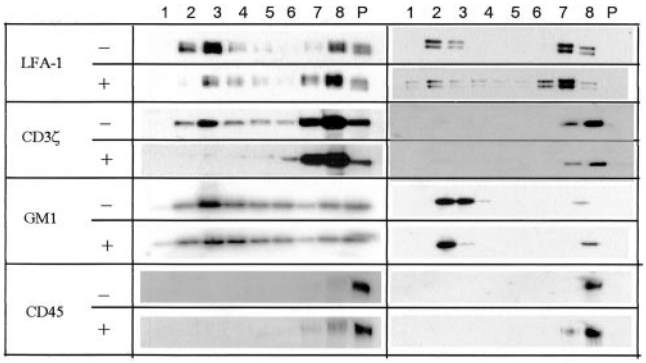

FIGURE 2. LFA-1 and CD3 are found in MCD-sensitive detergent-insoluble fractions. CTL (*left panel*) and resting primary splenic T cells (*right panel*) were incubated with 20 mM (for CTL) or 10 mM (for splenic T cells) $MCD^{+/+}$ or no $MCD^{-/-}$ as in Fig. 1, solubilized with ice-cold 1% Brij 35, and subjected to sucrose gradient centrifugation for 18 h at 4°C. Eight fractions were collected from top to bottom. Detergent-resistant light-density fractions are recovered in fractions 2 and 3, and material at the bottom were referred to as pellet (p). Indicated molecules in each fraction were detected by Western blot using anti-CD18 Ab, anti-CD3ζ Ab, biotinylated CtxB, and anti-CD45 Ab with anti-rat IgG secondary Abs or streptavidin conjugated with HRP and the ECL. The results are representative of three independent experiments.

MCD-sensitive. Thus, LFA-1 on resting T cells and CTL is similarly distributed in lipid rafts. In contrast, the distribution of CD3 on CTL was significantly different from that on resting T cells. Approximately 30% of CD3 on CTL was found in the low-density raft fractions, whereas no CD3 of resting T cells was found in the raft fractions. This is consistent with earlier studies reporting that TCR becomes associated with lipid rafts upon activation by Ab cross-linking (25). MCD treatment almost completely shifted CD3 in the raft fractions to nonraft fractions, indicating that cholesterol is critical for the integrity of the lipid rafts containing CD3. The distribution of GM1 was not affected by cholesterol depletion. CD45, which is not found in lipid rafts, was used as negative control. When Triton X-100 was used in place of Brij 35, GM1, but not CD3 or LFA-1, was found in detergent-insoluble low-density fractions, suggesting that the lipid rafts containing CD3 and LFA-1 are soluble in 1% Triton X-100. Thus, as we previously reported with resting T cells (4), lipid rafts of CTL are likely heterogeneous. Some lipid rafts of CTL contain a high amount of GM1 but are low in cholesterol and are resistant to cholesterol depletion, whereas those with a high amount of cholesterol but are low in GM1 are readily disrupted by MCD treatment. LFA-1 is found in both MCD-sensitive and MCD-resistant lipid rafts, whereas CD3 of CTL, but not resting T cells, is in MCD-sensitive lipid rafts that are thought to be cholesterol-rich.

LFA-1 and CD3 on CTL, but not resting T cells, cocap

The above results suggest that some LFA-1 and CD3ϵ on CTL may colocalize in lipid rafts. To confirm, we induced capping of LFA-1 on CTL by Ab cross-linking and examined the distribution of CD3ϵ. Both LFA-1 and CD3ϵ were evenly distributed on the surface of untreated CTL (Fig. 3, *row 1*). Cross-linking of LFA-1 (red) induced redistribution of virtually all LFA-1 to one side of the cells, forming a distinct "cap." This induced redistribution of CD3ϵ (green) to the same site, and the resultant codistribution of LFA-1 and CD3ϵ formed a yellow cap in the merged image. This cocapping was seen in 92 ± 5% ($n = 50$) of the cells examined. Conversely, when capping of CD3ϵ was induced by Ab cross-linking, some, but not all, LFA-1 cocapped with CD3ϵ in majority

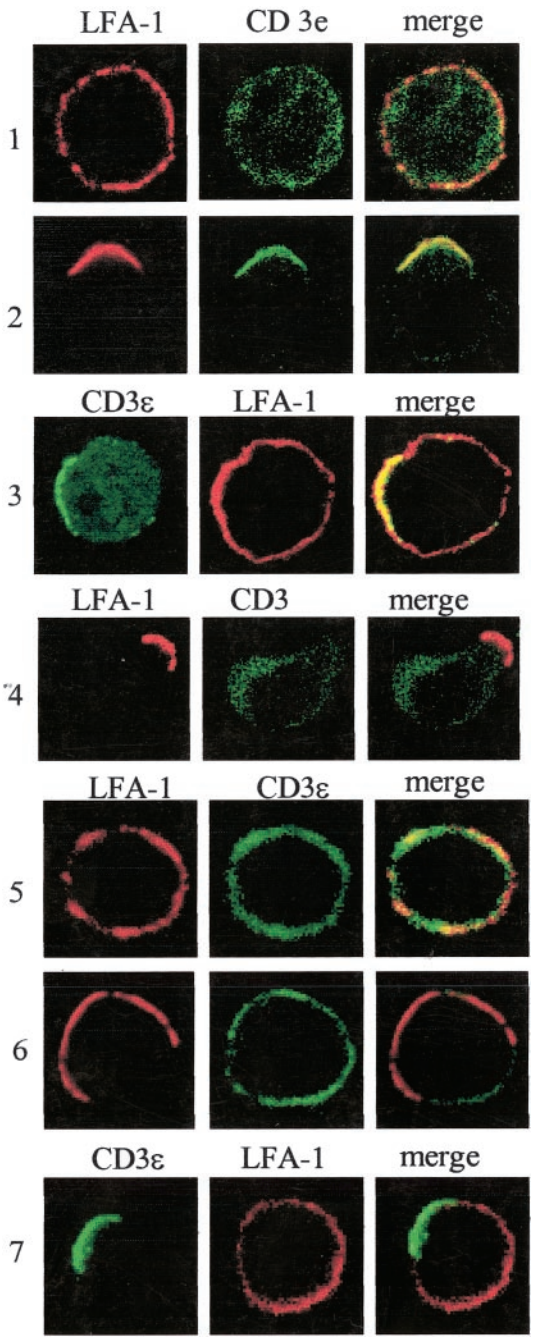

FIGURE 3. LFA-1 and CD3 cocap on CTL, but not on resting T cells. CTL (*rows 1-4*) and splenic T cells (*rows 5-7*) were untreated (*rows 1* and *5*) or incubated with either anti-LFA-1 (*rows 2* and *6*) or anti-CD3ϵ (*rows 3* and *7*) on ice for 30 min. After washing, appropriate secondary Abs were added for cross-linking and incubated at 37°C for 30 min. The cells were then fixed with 4% paraformaldehyde and stained with anti-CD3 or anti-LFA-1 where indicated. CTLs were also treated with 20 mM MCD for 30 min at 37°C, before LFA-1 capping by cross-linking, then fixed and stained for CD3ϵ, (*row 4*). The stained cells were examined by confocal microscope, and images at the middle sections of the cells were obtained. Each set of images is representative of 50 cells examined in three independent experiments.

(82 ± 7%; $n = 50$) of the cells examined (Fig. 3, *row 3*). It should be noted that LFA-1 is much more abundant than CD3ϵ on CTL, and some LFA-1 did not seem to associate with lipid rafts (see above). Treatment of CTL with MCD did not affect capping of LFA-1, induced by anti-LFA-1 mAb cross-linking, but it almost

completely (91 ± 4%; $n = 50$) inhibited cocapping of CD3ε with LFA-1 (Fig. 3, *row 4*). Therefore, lipid rafts seem to be important for the association between LFA-1 and CD3 on CTL. LFA-1 and CD3 on resting T cells showed very different distributions from those on CTL. Capping of LFA-1 on resting T cells did not cause cocapping of CD3ε (Fig. 3, *row 6*). Similarly, capping of CD3ε did not result in cocapping of LFA-1 on resting T cells (Fig. 3, *row 7*). These findings support the notion that LFA-1 and CD3 colocalize in the same membrane microdomains on CTL whereas they are in different microdomains on resting T cells.

LFA-1 and CD3 codistribute with cholesterol and GM1 on CTL

Ganglioside GM1 and cholesterol are two major components of lipid rafts. To examine the association of LFA-1 and CD3 with lipid rafts, we tested cocapping of LFA-1 and lipid rafts. CtxB was used to detect GM1, whereas cholesterol was stained with filipin III, a fluorescent compound derived from *Saccharomyces filipinensis* that is known to specifically bind to membrane cholesterol (26). Before cross-linking of LFA-1, GM1 and cholesterol were evenly distributed on the surface of CTL (Fig. 4, *row 1*). Cross-linking of LFA-1 induced cocapping of most, but not all, GM1 and cholesterol, forming a white cap in the merged image (Fig. 4, *row 2*) with most (92 ± 4%; $n = 50$) of the cells examined. Cross-linking of CD3 also induced its capping, but no detectable cocapping of GM1 and cholesterol was detected (88 ± 6%; $n = 40$; Fig. 4, *row 3*). It should be noted that the amount of CD3 on CTL is much lower than GM1 or cholesterol, and the area of capped CD3 was not devoid of cholesterol. Capping of GM1 induced cocapping of LFA-1 (Fig. 4, *row 5*) on most CTL (86 ± 5%; $n = 50$). In contrast, CD3 did not cocap with GM1 (Fig. 4, *row 7*) on most CTL (93 ± 3%; $n = 50$) and cholesterol did not cocap with GM1 (Fig. 4, *row 9*) on most CTL (95 ± 2%; $n = 50$). This is consistent with the notion that lipid rafts of CTL are heterogenous. It should be noted that the area of capped GM1 is not devoid of cholesterol suggesting that GM1-rich rafts contain a low amount of cholesterol.

LFA-1, CD3, and lipid rafts form the immunological synapse of CTL

The above results suggest that LFA-1 and CD3 colocalize in a subset of lipid rafts on CTL. To investigate the physiological significance of this finding, we examined the distribution of these molecules in the immunological synapse formed on CTL upon interaction with target cells. We generated TCR transgenic CTL specific for the H-Y peptide presented by D^b. Murine fibroblast line L cells ($H\text{-}2^k$), which lack expression of the LFA-1 ligand, ICAM-1, were transfected with ICAM-1 alone, D^b alone, and both D^b and ICAM-1 (Fig. 5*A*) and used as target cells. Prolonged incubation (over 30 min) of the CTL with the targets resulted in lysis of L cells expressing D^b and ICAM-1 pulsed with the H-Y peptide but not control peptide, whereas those expressing ICAM-1 alone or D^b alone were not killed (data not shown). The CTLs were centrifuged onto the transfected L cell monolayers, incubated for 5, 15, and 20 min, and fixed and stained for LFA-1, CD3, GM1, cholesterol, and tyrosine phosphorylated proteins. Differential interference contrast microscopy showed that the CTL formed tight cell contact with L cells transfected with D^b and ICAM-1 (Fig. 5*B*, *left panel*) or ICAM-1 alone (*right panel*), whereas the CTL did not bind to untransfected L cells or those transfected only with D^b, and they were not analyzed in this study. The distribution of various molecules on the CTL at the cell contact sites was further analyzed by deconvolution fluorescence microscopy and 3-D reconstruction of the florescence images (see *Materials and Methods*), and 18–20 images viewed en face from the CTL side were analyzed for each time point and CTL-target combination. For all

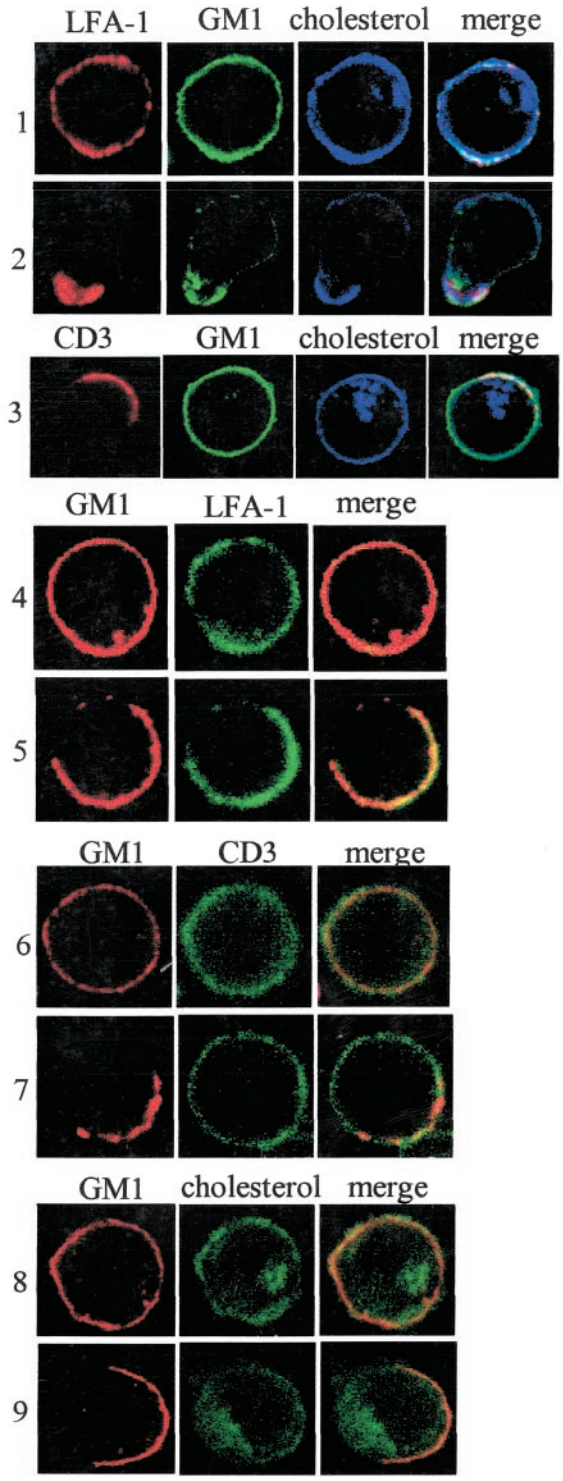

FIGURE 4. LFA-1 cocaps with both GM1 and cholesterol, but CD3 and cholesterol do not cocap with GM1. CTL were either untreated (*rows 1, 4, 6, 8*), treated to cross-link LFA-1 (*row 2*) and CD3ε (*row 3*) as in Fig. 3, or treated with FITC-CtxB and anti-Ctx Abs to cross-link GM1 (*rows 5, 7, 9*) for 30 min. They were then fixed and stained for indicated molecules. Filipin III (125 μg/ml) was used to stain cholesterol. The stained cells were analyzed by confocal microscopy as in Fig. 3. Each set of images is representative of 50 cells examined in two or three independent experiments. Over 90% of the cells showed similar stainings.

the molecules tested, no difference in their distribution was seen between the synapses formed when CTL bind to L cells expressing ICAM-1 and those with both ICAM-1 and D^b. The distribution of

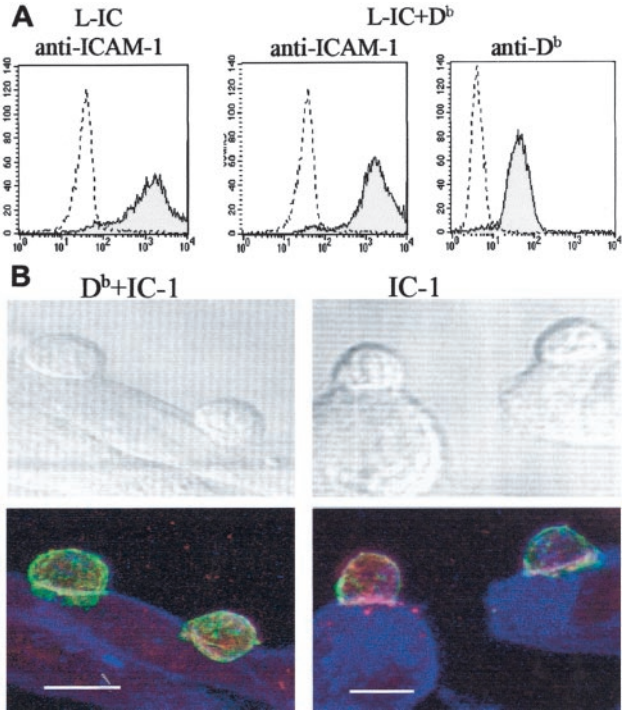

FIGURE 5. CTL tightly bind to L cells transfected with ICAM-1 or ICAM-1 and MHC class I D^b. *A*, L cells were transfected with ICAM-1 alone (L − IC) or with both MHC class I D^b and ICAM-1 (L − IC + D^b). The expression of D^b and ICAM-1 on the transfected cells was analyzed by flow cytometry. Solid histograms show ICAM-1 staining (*left* and *center*) or D^b staining (*right*) and open histograms show isotype control staining. These cells were used as a target for CTL in the immunological synapse experiments. *B*, L cells transfected with D^b and ICAM-1 (D^b + IC-1) or ICAM-1 alone (IC-1) were pulsed with H-Y peptide and incubated with H-Y-specific CTL for 5 min. They were then fixed and stained with filipin III for cholesterol (blue), FITC-CtxB for GM1 (green), and anti-LFA-1 (red). Top pictures show differential interference contrast images and bottom pictures show fluorescence staining. L cells express very low amounts of GM1 and are not stained with CtxB, but they express high amounts of cholesterol and are readily visualized by staining with filipin III.

LFA-1 (red) and GM1 (green) in the synapse was very similar to each other in most of the synapse analyzed and often formed yellow ring-like or partial ring distribution in the merged two-color images. In contrast, cholesterol (blue) distribution was often (but not always) quite different from those of LFA-1 and GM1. Fig. 6 shows representative images of CTL synapse where the target was transfected with ICAM-1 alone. Similar distribution was observed when the target was transfected with D^b and ICAM-1 (not shown). In some of the synapses, cholesterol (blue) was found in the center whereas LFA-1 (red) and GM1 (green) formed a ring in the peripheral (Fig. 6, *row 1*). This distribution was observed with ~30% ($n = 40$) of the CTL incubated for 5 min with the targets and was seen more often (~60%, $n = 36$) with those incubated for 15 or 20 min. Staining with CD3ϵ (green), GM1 (red), and cholesterol (blue) also showed the same patterns of distribution (Fig. 6, *row 2*). CD3 and GM1 colocalized, often forming yellow rings (*lower row*), while cholesterol (blue) showed mostly different patterns. Costaining with CD3 and LFA-1 further confirmed the codistribution of CD3 and LFA-1 in the synapse (Fig. 6, *row 3*). Distribution of these molecules on the CTL surface at noncell contact sites was also examined as controls and were found to be randomly distributed (Fig. 6, *row 4*). We also used the murine T cell line RMA ($H\text{-}2^b$) pulsed with the H-Y peptide as target and examined

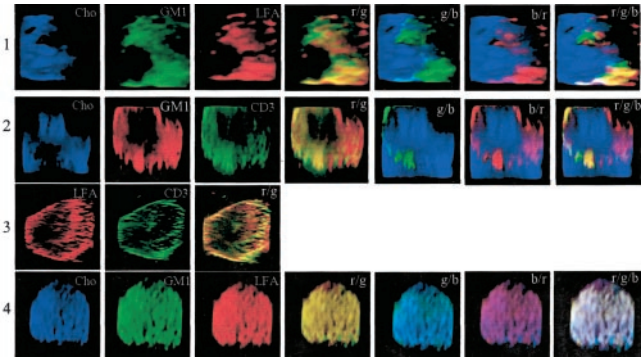

FIGURE 6. LFA-1, CD3, and lipid rafts form CTL immunological synapse. L cells transfected with ICAM-1 or D^b and ICAM-1 were pulsed with H-Y peptide and incubated with CTL. After incubation for 5, 15, or 20 min at 37°C cells, they were fixed and stained for GM1, LFA-1, CD3, and cholesterol. The stained cells were analyzed by a deconvolution microscope. The stacks were 3-D reconstructed, and the CTL-L cell interphase were cropped and rotated to obtain a view from the CTL side. In *row 1*, synapse was stained with filipin III for cholesterol (Cho; blue), CtxB-biotin and streptavidin-FITC for GM1 (green), and anti-LFA-1 and Alexa Fluor 568-conjugated secondary Ab (red). In *row 2*, staining with filipin III (blue), CtxB-biotin and streptavidin-Alexa Fluor 568 (red), and anti-CD3ϵ-FITC (green) is shown. In *row 3*, staining with anti-LFA-1 and Alexa Fluor 568-conjugated secondary Ab (red) and anti-CD3ϵ-FITC (green) is shown. In *row 4*, a section of the CTL membrane that was not making contact with L cells was stained as in *row 1*. The merged images of various color combinations (r, red; g, green; b, blue) are also shown. Each image is representative of 18–20 synapses examined for each condition of target cell (D^b + ICAM-1 or ICAM-1 alone), LFA-1 or CD3ϵ staining or both, and different incubation time course (5, 15, and 20 min). No difference was seen between the synapse formed when CTLs were incubated with L cells expressing ICAM-1 and those expressing ICAM-1 and D^b. Similar images were obtained with cells incubated for 5, 15, or 20 min, although the distribution patterns shown in this figure were seen less frequently with 5-min incubation.

the distribution of LFA-1, CD3ϵ, and GM1 on CTL, and the results were identical with those in Fig. 6 (results not shown).

Ag recognition by TCR initiates signaling and translocation of microtubule organization center (MTOC)

Because no obvious difference in the distribution of LFA-1, CD3, GM1, and cholesterol was seen between the synapses of the CTL incubated with L cells expressing ICAM-1 alone and those expressing D^b and ICAM-1, the formation of the immunological synapse on CTL seems to be Ag-independent and initiated by the interaction of LFA-1 on CTL to its ligand, ICAM-1, on target cells. When the distribution of tyrosine-phosphorylated proteins in the CTL was examined, a clear difference was found between the CTL incubated with L cells expressing ICAM-1 alone (Fig. 7*A*, *upper row*) and those expressing D^b and ICAM-1 (Fig. 7*A*, *lower row*), both of which were pulsed with H-Y peptide. In the former, tyrosine-phosphorylated proteins were detected throughout the cells, whereas they were highly localized at the cell contact site in the latter (Fig. 7*A*), indicating that the TCR/CD3 complex in the synapse, upon interaction with appropriate peptide/MHC, triggers activation signals and induces highly localized signaling events at the synapse. We also tested the distribution of tubulin and MTOC (Fig. 7*B*, indicated by arrows). When CTL recognized the peptide-pulsed target cells expressing ICAM-1 and D^b (L − IC + D^b), MTOC was reoriented toward the target cells. This pattern was observed in 83% of the conjugates ($n = 54$). When CTL interacted with target cells expressing ICAM-1 alone (L − IC) in an Ag-independent manner, MTOC was found to be distributed elsewhere. This was observed in 82% of the conjugates ($n = 44$).

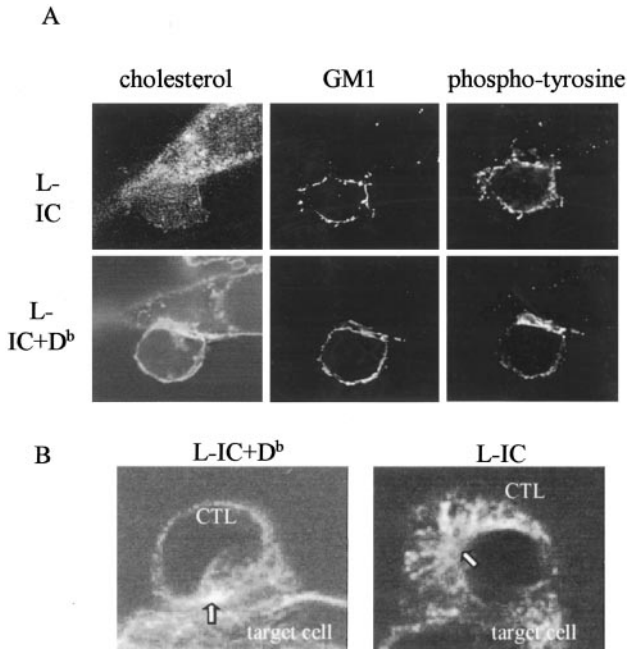

FIGURE 7. *A*, Tyrosine-phosphorylated proteins and MTOC accumulate in Ag-specific CTL synapse. CTL were incubated with H-Y peptide-pulsed L cells transfected with ICAM-1 (L − IC) or ICAM-1 and D^b (L − IC + D^b) for 5 min, fixed, permeabilized, and stained for indicated molecules. Cholesterol and GM1 were stained as in Fig. 6, whereas phospho-tyrosine was stained with the anti-phospho-tyrosine mAb 4G10 and Alexa Fluor 568-conjugated secondary Ab. The stained cells were analyzed by deconvolution microscope. Images at the midsection of the CTL are shown. The images are representative of >40, all showing similar patterns of staining for each condition. *B*, Target cells (L − IC and L − IC + D^b) were incubated with CTL and both were stained for β-tubulin with anti-mouse β-tubulin and Alexa Fluor 568-conjugated secondary Ab.

These results demonstrate that ligation of LFA-1 on CTL is not sufficient for the initiation of activation signals or the MTOC reorientation toward CTL synapse, and the recognition of cognate peptide/MHC by TCR is required for CTL activation.

Discussion

We have demonstrated that LFA-1 and CD3 on CTL colocalize in lipid rafts. When CTL bind to target cells, both CD3 and LFA-1 are distributed to the periphery of the cell contact site. This pattern is in contrast to that in the immunological synapse formed on $CD4^+$ T cells interacting with APCs (7–9). In the latter synapse, the TCR and LFA-1 show differential distribution. Initially, LFA-1 distributes in the center of the synapse surrounded by the TCR, whereas mature synapse has the TCR in the center and LFA-1 in the periphery. Furthermore, the formation of the CTL synapse is Ag-independent, whereas the recognition of specific peptide-MHC complex by the TCR is essential for the formation of the immunological synapse on $CD4^+$ T cells, although Ag-independent synapse on CD4 T cells interacting with dendritic cells has been reported (27). These differences between the immunological synapse of CTL and that on resting CD4 T cells are likely due to differences in the distribution and activation status of LFA-1 and CD3 on these cells. LFA-1 on CTL is functionally active and readily mediates cell adhesion to ICAM-1, whereas LFA-1 on resting T cells is an inactive form and has to be activated to mediate cell adhesion. Moreover, some CD3 on CTL is found in cold, detergent-insoluble light-density fractions, whereas no CD3 on resting T cells was detected in the same fractions. Cross-linking of LFA-1 on CTL induces cocapping of LFA-1, CD3, GM1, and cholesterol, whereas no cocapping of LFA-1 and CD3 was induced with resting T cells. GM1 and cholesterol are thought to be major components of lipid rafts, and the cocapping of LFA-1 and CD3 is inhibited by cholesterol depletion with MCD. Therefore, these results suggest that LFA-1 and CD3 on CTL colocalize in lipid rafts of CTL, whereas CD3 on resting T cells is not in lipid rafts and not associated with LFA-1. It appears that binding of functionally active LFA-1 on CTL to ICAM-1 on target cells initiates accumulation of LFA-1 in the cell contact site and brings the TCR/CD3 complex that associates with LFA-1 through lipid rafts to the cell contact site forming the CTL synapse. The inhibition of cytotoxicity by MCD treatment may be due to inhibition of TCR-mediated calcium signaling as reported by Doucey et al. (24). However, MCD treatment also disrupts the association between LFA-1 and CD3 and may inhibit localization of CD3 in the synapse. It is possible that MCD inhibits LFA-1-mediated signaling. The association of LFA-1 and CD3 on CTL implies that the recruitment of the TCR/CD3 complex to the synapse is highly efficient and Ag-independent. The TCR recruited to the synapse would scan the MHC-peptide complex on target cells and transduce activation signals upon interaction with cognate peptide-MHC and result in reorientation of tubulin and MTOC (Fig. 7, *A* and *B*). This would be followed by the movement of lytic granules along the microtubule and docked within the secretory domain of the immunological synapse mediated by adaptor protein-3 (28, 29). The association of CD3 and LFA-1 with lipid rafts on CTL also suggests that activation complexes consisting of the TCR, LFA-1, and signaling molecules such as the Src family of protein tyrosine kinases, which are also found in lipid rafts, might be preassembled, which would result in rapid activation of CTL upon encountering target cells expressing cognate peptide-MHC complex. Indeed, activation of CTL as indicated by exocytosis of cytotoxic granules, is rapid and takes only minutes following binding to target cells. In contrast, activation of resting T cells requires prolonged interaction with APCs (9–11, 13, 30). The formation of the immunological synapse on resting T cells is also rather complex. It requires functional activation of LFA-1, recognition of cognate peptide/MHC complex, and recruitment of lipid rafts and signaling molecules (9).

Our results are in general agreement with recent reports of the CTL immunological synapse. Using supported planar lipid bilayer containing ICAM-1, Somersalo et al. (31) have reported that human CTL clones form an Ag-independent ring junction of LFA-1. Although the distribution of the TCR and GM1 in the CTL synapse in their report is different from that in our study, it maybe due to differences in the targets (cells vs planar membranes). Stinchcombe at al. (15) have reported that CTL forms mature synapse with adhesion molecules forming a ring surrounding an inner signaling domain. However, the distribution of the CD3/TCR complex was not directly examined in their study. Faroudi et al. (32) reported that multiple molecules, including CD2, phosphotyrosine, tubulin, and perforin, accumulate at the CTL-target interphase in an Ag-dependent manner, but the distribution of LFA-1 and CD3 in the synapse was not studied (32). Purbhoo et al. (33) have recently examined the distribution of MHC/peptide and ICAM-1 on target cells as they interact with CTL and found that a ring-like distribution of ICAM-1 in the synapse is dependent on accumulation of a high level of MHC/peptide, whereas CTL killing requires only three MHC/peptide complexes, suggesting that formation of a stable synapse is not required for CTL killing.

It has been suggested that CD3 and LFA-1 have to be physically separated in the immunological synapse to allow binding to their respective ligands, because LFA-1 and ICAM-1 are considerably larger than the TCR and MHC. Thus, codistribution of LFA-1 and

CD3 may cause physical constraints to their ligand binding. However, LFA-1 on CTL seems to be already activated and its conformation may be significantly different from that of inactive LFA-1 on resting T cells. Crystal structure studies have shown that the ligand-bound integrin, $\alpha_V\beta_3$, has a bent structure (34, 35). This bending substantially reduces its height on the surface of the plasma membrane. ICAM-1 also has a 90° bend in its structure at its 3rd and 4th Ig-like domains. It is estimated that the binding of bent LFA-1 to ICAM-1 will generate ~15 nm of separation between the membranes of two interacting cells. This may allow TCR to interact with MHC, which is thought to require a distance of 15 nm or less between them (8). Thus, codistribution of LFA-1 and CD3 in the CTL synapse may facilitate the binding of the TCR/CD3 complex to MHC-peptide. It remains to be determined whether activated LFA-1 on the cell surface exists in a bent form or an extended form, as suggested by electron micrographs of purified soluble LFA-1 (36).

Our results suggest that some LFA-1 and CD3 on CTL localize in membrane microdomains rich in cholesterol and ganglioside GM1. In the plasma membrane, cholesterol and GM1 are thought to cluster and form liquid-ordered microdomains, termed lipid rafts. Because these putative microdomains are too small for optical microscopy, the existence of lipid rafts in intact cells is difficult to demonstrate, and whether they actually form unique microdomains on intact cells has been questioned (37). In our study, we used a combination of density separation of cold, nonionic detergent-insoluble membranes, cholesterol depletion, and cocapping experiments to demonstrate that LFA-1 somehow associates with CD3, cholesterol, and GM1 on the surface of CTL. Interestingly, cross-linking of GM1 induces cocapping of some LFA-1, but not cholesterol, suggesting that GM1 and cholesterol may not necessarily coexist in the same microdomains. This is consistent with our previous results that suggested a heterogeneity of lipid rafts of primary T cells (4).

In the CTL synapse, GM1 mainly colocalizes in the periphery with LFA-1 and CD3, whereas cholesterol is more widely distributed, including the center of the synapse. This distribution of GM1 in the CTL synapse is different from that in the immunological synapse of resting CD4 T cells. In the latter, GM1 is enriched in the center of the synapse (17), again reflecting significant differences between these two types of immunological synapses. It is currently unknown why the distribution of cholesterol is different from that of CD3, LFA-1, and GM1 in the CTL synapse, but it seems likely that cholesterol-rich lipid rafts may contain unidentified molecules that participate in the formation of the synapse.

Acknowledgments

We thank Nastaran Mohammadi for technical assistance and Motoi Maeda for discussions.

References

1. Simons, K., and R. Ehehalt. 2002. Cholesterol, lipid rafts, and disease. *J. Clin. Invest. 110:597*.
2. Dykstra, M., A. Cherukuri, H. W. Sohn, S. J. Tzeng, and S. K. Pierce. 2003. Location is everything: lipid rafts and immune cell signaling. *Annu. Rev. Immunol. 21:457*.
3. Schade, A. E., and A. D. Levine. 2002. Lipid raft heterogeneity in human peripheral blood T lymphoblasts: a mechanism for regulating the initiation of TCR signal transduction. *J. Immunol. 168:2233*.
4. Marwali, M. R., J. Rey-Ladino, L. Dreolini, D. Shaw, and F. Takei. 2003. Membrane cholesterol regulates LFA-1 function and lipid raft heterogeneity. *Blood 102:215*.
5. Gomez-Mouton, C., J. L. Abad, E. Mira, R. A. Lacalle, E. Gallardo, S. Jimenez-Baranda, I. Illa, A. Bernad, S. Manes, and A. Martinez. 2001. Segregation of leading-edge and uropod components into specific lipid rafts during T cell polarization. *Proc. Natl. Acad. Sci. USA 98:9642*.
6. Montoya, M. C., D. Sancho, M. Vicente-Manzanares, and F. Sanchez-Madrid. 2002. Cell adhesion and polarity during immune interactions. *Immunol. Rev. 186:68*.
7. Bromley, S. K., W. R. Burack, K. G. Johnson, K. Somersalo, T. N. Sims, C. Sumen, M. M. Davis, A. S. Shaw, P. M. Allen, and M. L. Dustin. 2001. The immunological synapse. *Annu. Rev. Immunol. 19:375*.
8. Sims, T. N., and M. L. Dustin. 2002. The immunological synapse: integrins take the stage. *Immunol. Rev. 186:100*.
9. Huppa, J. B., and M. M. Davis. 2003. T-cell-antigen recognition and the immunological synapse. *Nat. Rev. Immunol. 3:973*.
10. Freiberg, B. A., H. Kupfer, W. Maslanik, J. Delli, J. Kappler, D. M. Zaller, and A. Kupfer. 2002. Staging and resetting T cell activation in SMACs. *Nat. Immunol. 3:911*.
11. Lee, K. H., A. D. Holdorf, M. L. Dustin, A. C. Chan, P. M. Allen, and A. S. Shaw. 2002. T cell receptor signaling precedes immunological synapse formation. *Science 295:1539*.
12. Lee, S. J., Y. Hori, J. T. Groves, M. L. Dustin, and A. K. Chakraborty. 2002. Correlation of a dynamic model for immunological synapse formation with effector functions: two pathways to synapse formation. *Trends Immunol. 23:492*.
13. Huppa, J. B., M. Gleimer, C. Sumen, and M. M. Davis. 2003. Continuous T cell receptor signaling required for synapse maintenance and full effector potential. *Nat. Immunol. 4:749*.
14. Wulfing, C., C. Sumen, M. D. Sjaastad, L. C. Wu, M. L. Dustin, and M. M. Davis. 2002. Costimulation and endogenous MHC ligands contribute to T cell recognition. *Nat. Immunol. 3:42*.
15. Stinchcombe, J. C., G. Bossi, S. Booth, and G. M. Griffiths. 2001. The immunological synapse of CTL contains a secretory domain and membrane bridges. *Immunity 15:751*.
16. Bossi, G., C. Trambas, S. Booth, R. Clark, J. Stinchcombe, and G. M. Griffiths. 2002. The secretory synapse: the secrets of a serial killer. *Immunol. Rev. 189:152*.
17. Burack, W. R., K. H. Lee, A. D. Holdorf, M. L. Dustin, and A. S. Shaw. 2002. Cutting edge: quantitative imaging of raft accumulation in the immunological synapse. *J. Immunol. 169:2837*.
18. Dupre, L., A. Aiuti, S. Trifari, S. Martino, P. Saracco, C. Bordignon, and M. G. Roncarolo. 2002. Wiskott-Aldrich syndrome protein regulates lipid raft dynamics during immunological synapse formation. *Immunity 17:157*.
19. Viola, A., S. Schroeder, Y. Sakakibara, and A. Lanzavecchia. 1999. T lymphocyte costimulation mediated by reorganization of membrane microdomains. *Science 283:680*.
20. Takei, F. 1985. Inhibition of mixed lymphocyte response by a rat monoclonal antibody to a novel murine lymphocyte activation antigen (MALA-2). *J. Immunol. 134:1403*.
21. Welder, C. A., D. H. Lee, and F. Takei. 1993. Inhibition of cell adhesion by microspheres coated with recombinant soluble intercellular adhesion molecule-1. *J. Immunol. 150:2203*.
22. Lian, R. H., Y. Li, S. Kubota, D. L. Mager, and F. Takei. 1999. Recognition of class I MHC by NK receptor Ly-49C: identification of critical residues. *J. Immunol. 162:7271*.
23. Simons, K., and D. Toomre. 2000. Lipid rafts and signal transduction. *Nat. Rev. Mol. Cell. Biol. 1:31*.
24. Doucey, M. A., D. F. Legler, N. Boucheron, J. C. Cerottini, C. Bron, and I. F. Luescher. 2001. CTL activation is induced by cross-linking of TCR/MHC-peptide-CD8/p56^{lck} adducts in rafts. *Eur. J. Immunol. 31:1561*.
25. Xavier, R., T. Brennan, Q. Li, C. McCormack, and B. Seed. 1998. Membrane compartmentation is required for efficient T cell activation. *Immunity 8:723*.
26. Hassall, D. G., and A. Graham. 1995. Changes in free cholesterol content, measured by filipin fluorescence and flow cytometry, correlate with changes in cholesterol biosynthesis in THP-1 macrophages. *Cytometry 21:352*.
27. Revy, P., M. Sospedra, B. Barbour, and A. Trautmann. 2001. Functional antigen-independent synapses formed between T cells and dendritic cells. *Nat. Immunol. 2:925*.
28. Kuhn, J. R., and M. Poenie. 2002. Dynamic polarization of the microtubule cytoskeleton during CTL-mediated killing. *Immunity 16:111*.
29. Clark, R. H., J. C. Stinchcombe, A. Day, E. Blott, S. Booth, G. Bossi, T. Hamblin, E. G. Davies, and G. M. Griffiths. 2003. Adaptor protein 3-dependent microtubule-mediated movement of lytic granules to the immunological synapse. *Nat. Immunol. 4:1111*.
30. Schrum, A. G., and L. A. Turka. 2002. The proliferative capacity of individual naive CD4$^+$ T cells is amplified by prolonged T cell antigen receptor triggering. *J. Exp. Med. 196:793*.
31. Somersalo, K., N. Anikeeva, T. N. Sims, V. K. Thomas, R. K. Strong, T. Spies, T. Lebedeva, Y. Sykulev, and M. L. Dustin. 2004. Cytotoxic T lymphocytes form an antigen-independent ring junction. *J. Clin. Invest. 113:49*.
32. Faroudi, M., C. Utzny, M. Salio, V. Cerundolo, M. Guiraud, S. Muller, and S. Valitutti. 2003. Lytic versus stimulatory synapse in cytotoxic T lymphocyte/target cell interaction: manifestation of a dual activation threshold. *Proc. Natl. Acad. Sci. USA 100:14145*.
33. Purbhoo, M. A., D. J. Irvine, J. B. Huppa, and M. M. Davis. 2004. T cell killing does not require the formation of a stable mature immunological synapse. *Nat. Immunol. 5:524*.
34. Xiong, J. P., T. Stehle, B. Diefenbach, R. Zhang, R. Dunker, D. L. Scott, A. Joachimiak, S. L. Goodman, and M. A. Arnaout. 2001. Crystal structure of the extracellular segment of integrin $\alpha_V\beta_3$. *Science 294:339*.
35. Xiong, J. P., T. Stehle, R. Zhang, A. Joachimiak, M. Frech, S. L. Goodman, and M. A. Arnaout. 2002. Crystal structure of the extracellular segment of integrin $\alpha_V\beta_3$ in complex with an Arg-Gly-Asp ligand. *Science 296:151*.
36. Takagi, J., and T. A. Springer. 2002. Integrin activation and structural rearrangement. *Immunol. Rev. 186:141*.
37. Munro, S. 2003. Lipid rafts: elusive or illusive? *Cell 115:377*.